HHS Public Access

Author manuscript

Immunity. Author manuscript; available in PMC 2018 November 21.

Published in final edited form as:

Immunity. 2017 November 21; 47(5): 890–902.e4. doi:10.1016/j.immuni.2017.10.021.

Granulocyte-monocyte progenitors and monocyte-dendritic cell progenitors independently produce functionally distinct monocytes

Alberto Yáñez[1,2], **Simon G. Coetzee**[2,3], **Andre Olsson**[4], **David E. Muench**[4], **Benjamin P. Berman**[2,3], **Dennis J. Hazelett**[2,3], **Nathan Salomonis**[5], **H. Leighton Grimes**[4,6], and **Helen S. Goodridge**[1,2]

[1]Board of Governors Regenerative Medicine Institute

[2]Department of Biomedical Sciences

[3]Bioinformatics and Computational Biology Research Center, Cedars-Sinai Medical Center, 8700 Beverly Boulevard, Los Angeles, CA 90048, USA

[4]Division of Immunobiology and Center for Systems Immunology

[5]Division of Biomedical Informatics

[6]Division of Experimental Hematology and Cancer Biology, Cincinnati Children's Hospital Medical Center, Cincinnati, Ohio, 45229, USA

Summary

Granulocyte-monocyte progenitors (GMPs) and monocyte-dendritic cell progenitors (MDPs) produce monocytes during homeostasis and in response to increased demand during infection. Both progenitor populations are thought to derive from common myeloid progenitors (CMPs), and a hierarchical relationship (CMP-GMP-MDP-monocyte) is presumed to underlie monocyte differentiation. Here, however, we demonstrate that mouse MDPs arose from CMPs independently of GMPs, and that GMPs and MDPs produced monocytes via similar, but distinct, monocyte-committed progenitors. GMPs and MDPs yielded classical (Ly6C^{hi}) monocytes with gene expression signatures that were defined by their origins and impacted their function. GMPs produced a subset of "neutrophil-like" monocytes, whereas MDPs gave rise to a subset of monocytes that yielded monocyte-derived dendritic cells. GMPs and MDPs were also independently mobilized to produce specific combinations of myeloid cell types following the

Corresponding Author (Lead Contact): Helen S. Goodridge, Ph.D., Board of Governors Regenerative Medicine Institute, Cedars-Sinai Medical Center, 8700 Beverly Boulevard, Los Angeles, CA 90048, USA, Tel. +1-310-248-8577, helen.goodridge@csmc.edu.

Author Contributions

AY, SGC, BPB, DJH, NS, HLG, and HSG designed the study. AY, AO and DEM performed the *in vitro* and *in vivo* experiments, and AY, HLG and HSG analyzed the data. SGC, DJH and NS performed the gene expression data analyses. AY and HSG wrote the manuscript, and the other authors helped edit the manuscript.

Supplemental Information

Document S1. Figures S1–S7

injection of microbial components. Thus, the balance of GMP and MDP differentiation shapes the myeloid cell repertoire during homeostasis and following infection.

Graphical Abstract

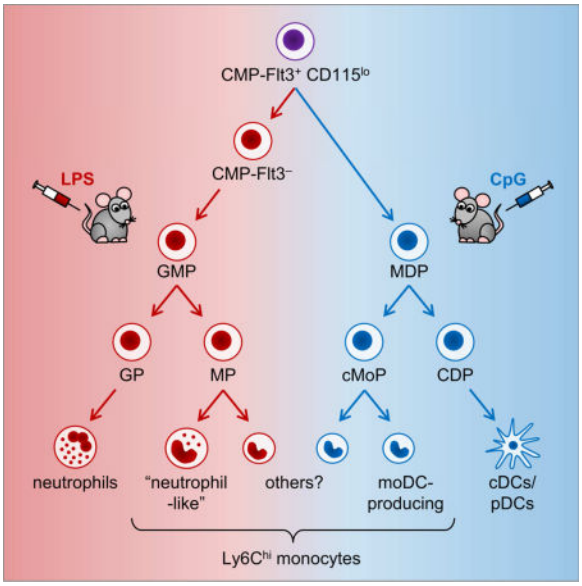

Introduction

Myeloid cells – neutrophils, monocytes, macrophages and dendritic cells (DCs) – play key roles in anti-microbial defense and inflammation, as well as tissue repair and remodeling. Recent studies have demonstrated that some tissue-resident macrophage populations (such as microglia in the brain) arise in the yolk sac during early embryogenesis and populate the tissues of the developing embryo, where they can be maintained by self-renewal for long periods (even throughout life) (Hashimoto et al., 2013; Schulz et al., 2012). Other tissue-resident macrophage populations arise from circulating monocytes produced by hematopoietic stem cells (HSCs), initially in the fetal liver and subsequently in the bone marrow (Geissmann and Mass, 2015; McGrath et al., 2015). Neutrophils and DCs are also derived from HSCs.

HSCs, like other stem cell populations, possess self-renewal properties and the ability to produce diverse progeny. Hematopoietic cells of 3 main lineages – erythroid, myeloid and lymphoid – are derived from HSCs via intermediate progenitors. In the steady-state, hematopoietic stem and progenitor cells (HSPCs) supply myeloid cells to tissues for immune surveillance and also maintain reserves in the bone marrow that can be dispatched quickly when a threat is detected. Under emergency conditions, such as during an active infection, the demand for myeloid cells (especially neutrophils and monocytes) increases. Myelopoiesis rates are adjusted accordingly to meet the additional need for innate immune cells and replenish depleted reserves, while differentiation via the erythroid and lymphoid lineages is temporarily scaled back.

Inflammatory cytokines and microbial components control the mobilization of specific HSPCs to direct the production of specific myeloid subsets during emergency myelopoiesis (Manz and Boettcher, 2014; Yanez et al., 2013). For instance, *Listeria monocytogenes* infection favors a predominantly monopoietic emergency response (Serbina et al., 2009), while *Candida albicans* infection induces both emergency granulopoiesis and monopoiesis (Basu et al., 2000; Yanez et al., 2011).

The classical model of hematopoiesis describes the production of diverse hematopoietic cells by multipotent HSCs via a series of progenitors with more restricted lineage potential. Granulocytes (including neutrophils), monocytes and DCs are thought to be produced by granulocyte-monocyte progenitors (GMPs) and monocyte-DC progenitors (MDPs), which are themselves derived from common myeloid progenitors (CMPs) (reviewed in (Zhu et al., 2016). However, recent studies have challenged hierarchical models of hematopoiesis and instead suggested that progenitors make lineage commitment decisions at an earlier stage than previously thought (Notta et al., 2016; Paul et al., 2015). A hybrid of these two scenarios is also possible, with some early progenitors losing multipotency and immediately adopting a particular fate, and others undergoing progressive lineage restriction under the control of competing transcriptional programs (Drissen et al., 2016; Olsson et al., 2016).

Two major types of monocytes have been reported in mice and humans (Geissmann et al., 2003; Passlick et al., 1989), although single-cell transcriptome profiling studies have recently revealed additional heterogeneity (Menezes et al., 2016; Villani et al., 2017). In mice, the most notable distinction is between classical or inflammatory monocytes, which strongly express Ly6C, and non-classical monocytes (including patrolling monocytes), which lack Ly6C (Carlin et al., 2013; Geissmann et al., 2003; Zhu et al., 2016). Classical monocyte fate is specified by the sequential expression of PU.1, IRF8 and Klf4 transcription factors (Zhu et al., 2016). Non-classical monocytes are thought to derive from classical monocytes under the control of Nur77 (NR4A1), although some investigators have questioned whether all non-classical monocytes arise by conversion of classical monocytes (reviewed in (Zhu et al., 2016)).

MDPs have recently been shown to yield monocyte-committed progenitors, named common monocyte progenitors (cMoPs), that produce both classical and non-classical monocytes (Hettinger et al., 2013). MDPs are widely thought to be derived from GMPs, because both GMPs and MDPs yield monocytes, while MDPs do not give rise to neutrophils (Akashi et al., 2000; Fogg et al., 2006; Hettinger et al., 2013; Yanez et al., 2015). In support of this model, MDP-derived cMoPs (Hettinger et al., 2013) and monocyte-committed progenitors produced by GMPs (named MPs; (Yanez et al., 2015)) appear to be the same cells (on the basis of shared surface marker expression), and adoptively transferred MDPs yield monocytes more rapidly than GMPs (Hettinger et al., 2013; Yanez et al., 2015). However, the relationship between GMPs and MDPs has never been formally evaluated. We therefore decided to test the hierarchical model of monocyte differentiation (CMP-GMP-MDP-MP/cMoP-monocyte).

In this study we demonstrate that GMPs (defined as Lin^{-} c-Kit^{+} Sca-1^{-} $CD34^{+}$ $Fc\gamma R^{hi}$ $Ly6C^{-}$ $Flt3^{-}$ $CD115^{lo}$ cells) from mouse bone marrow did not give rise to MDPs (defined as

Lin^{-} c-Kit^{+} Sca-1^{-} CD34^{+} FcγR^{lo} Flt3^{+} CD115^{hi} cells). Moreover, GMPs produced neutrophils and monocytes but not DCs, whereas MDPs yielded monocytes and DCs but not neutrophils. We show that GMPs and MDPs produced functionally distinct Ly6C^{hi} monocytes, and demonstrate differential mobilization of GMPs and MDPs to produce Ly6C^{hi} monocytes (and either neutrophils or DCs) in response to diverse microbial stimuli.

Results

MDPs are not derived from GMPs, but both produce monocytes

GMPs and MDPs are thought to derive sequentially from a subset of CMPs that express Flt3 (Drissen et al., 2016; Guo et al., 2013; Onai et al., 2013). However, this relationship has not been confirmed and the lack of Flt3 expression by GMPs seemed inconsistent with their presumed position as intermediate progenitors between CMPs and MDPs, which are both Flt3^{+}. We therefore re-evaluated the assumption that a hierarchical relationship exists between CMPs, GMPs and MDPs.

We first verified the identity of the GMP and MDP fractions in mouse bone marrow by applying an unsupervised clustering method (viSNE; (Amir el et al., 2013)) to identify subsets of myeloid progenitors using a panel of 7 surface markers detected by flow cytometry. “GMPs” were originally defined as LKS^{-} CD34^{+} FcγR^{hi} cells (Akashi et al., 2000). However, in addition to progenitors with dual granulocyte-monocyte potential (oligopotent or multi-lineage GMPs), this fraction contains granulocyte-committed progenitors (GPs) and monocyte-committed progenitors (MPs or cMoPs) (Akashi et al., 2000; Hettinger et al., 2013; Olsson et al., 2016; Yanez et al., 2015), which we recently reported can be separated on the basis of their expression of Ly6C and CD115 (GMPs are Ly6C^{-} CD115^{lo}, GPs are Ly6C^{+} CD115^{lo}, and MPs are Ly6C^{+} CD115^{hi} (Yanez et al., 2015)). As expected, viSNE analysis confirmed the presence of subsets corresponding to GMPs, GPs and MPs/cMoPs in the LKS^{-} CD34^{+} FcγR^{hi} fraction of mouse bone marrow (Figure S1A–B).

MDPs were originally described as CX3CR1^{+} Flt3^{+} CD115^{+} cells in the LKS^{-} fraction of mouse bone marrow (Auffray et al., 2009; Fogg et al., 2006). viSNE analysis revealed that Flt3^{+} CD115^{+} cells predominantly expressed low amounts of FcγR (Figure S1A), which is consistent with the presence of MDPs in the FcγR^{lo} (“CMP”) gate (Figure S1B), rather than the FcγR^{hi} (“GMP”) gate as previously suggested (Fogg et al., 2006). Recent single-cell RNA sequencing studies have also suggested that DC progenitors are predominantly found in the “CMP” gate, rather than the “GMP” gate (Olsson et al., 2016; Paul et al., 2015). We confirmed that LKS^{-} CD34^{+} FcγR^{lo} Flt3^{+} CD115^{hi} cells strongly expressed CX3CR1 (Figure S1C), consistent with the presence of MDPs in this fraction.

Using these gating strategies to isolate the progenitor populations (Figures S1B, D and S2A), we first evaluated colony formation by the GMPs and MDPs in methylcellulose cultures that support the differentiation of neutrophils and monocytes (but not DCs). As expected, the MDP fraction predominantly yielded pure monocyte colonies, while the GMP fraction produced mixed granulocyte-monocyte colonies (Figure S2B). *In vivo* adoptive transfer into non-irradiated recipients confirmed that the MDP fraction gives rise to

monocytes and DCs (both cDCs and pDCs), but not neutrophils (Figures 1A and S3A). In contrast, however, adoptively transferred GMPs yielded neutrophils and monocytes, but no DCs, which suggested that MDPs may not be derived from GMPs (Figures 1A and S3A). Consistent with this, we did not observe MDP production by adoptively transferred GMPs (Figure 1B). Collectively these data demonstrate that MDPs are not derived from GMPs (which lack DC potential), and that monocytes are produced independently by both GMPs and MDPs, via MPs and cMoPs respectively. In *in vitro* cultures with M-CSF to drive monopoiesis, GMPs sequentially upregulated Ly6C and then CD115 when they differentiated to produce MPs, whereas MDPs (which already strongly expressed CD115) upregulated Ly6C when they gave rise to cMoPs (Figure S2C–E and data not shown).

We next investigated the upstream origins of GMPs and MDPs. The “CMP” fraction of mouse bone marrow (LKS^- $CD34^+$ $Fc\gamma R^{lo}$ cells), from which GMPs and MDPs are thought to derive, comprises a heterogeneous collection of progenitors with the potential to produce combinations of granulocytes, monocytes, DCs, megakaryocytes and erythrocytes (D’Amico and Wu, 2003; Drissen et al., 2016; Guo et al., 2013; Pronk et al., 2007). DC potential in the CMP fraction was previously shown to be restricted to a subset of cells expressing Flt3, while both the $Flt3^+$ and $Flt3^-$ fractions contain progenitors with the ability to produce neutrophils and monocytes (D’Amico and Wu, 2003). We isolated the $Flt3^+$ $CD115^{lo}$ (i.e. excluding MDPs, which are $Flt3^+$ $CD115^{hi}$) and $Flt3^-$ subsets (CMP-$Flt3^+$ $CD115^{lo}$ and CMP-$Flt3^-$ respectively; Figure S1B) and assessed their lineage potential. As expected, upon adoptive transfer into non-irradiated recipient mice, both CMP-$Flt3^+$ $CD115^{lo}$ and CMP-$Flt3^-$ cells yielded neutrophils and monocytes, but only CMP-$Flt3^+$ $CD115^{lo}$ cells produced DCs (Figures 1C and S3B). The CMP-$Flt3^-$ cells yielded neutrophils more rapidly than the CMP-$Flt3^+$ $CD115^{lo}$ cells (Figures 1C and S3B), which suggested that the CMP-$Flt3^-$ cells might represent a later progenitor stage. Consistent with this, methylcellulose cultures revealed that while both fractions predominantly comprised multi-lineage progenitors that were capable of producing erythrocytes and megakaryocytes as well as myeloid cells, the CMP-$Flt3^-$ fraction also contained progenitors that were already committed to erythrocyte and/or megakaryocyte production (Figure S3C).

We then used the adoptive transfer approach to investigate which myeloid progenitors are derived from the CMP-$Flt3^+$ $CD115^{lo}$ and CMP-$Flt3^-$ cells. Both fractions yielded GMPs, but only CMP-$Flt3^+$ $CD115^{lo}$ cells gave rise to MDPs, consistent with the inability of the CMP-$Flt3^-$ cells to produce DCs (Figure 1D). Moreover, the CMP-$Flt3^+$ $CD115^{lo}$ fraction yielded CMP-$Flt3^-$ cells (Figure 1D). Together, our data indicate that monocytes arise from CMP-$Flt3^+$ $CD115^{lo}$ cells via two separate pathways: 1) via CMP-$Flt3^-$ cell-derived GMPs, and 2) via MDPs, which arise independently of both CMP-$Flt3^-$ cells and GMPs (Figure S3D).

GMPs and MDPs produce both $Ly6C^{hi}$ and $Ly6C^-$ monocytes

We next considered why there might be two routes of monocyte differentiation. One possibility is that GMPs and MDPs yield different types of monocytes. In agreement with previous reports (Hettinger et al., 2013; Ingersoll et al., 2010), we identified 2 major subsets of cells expressing CD11b and CD115, but not Ly6G or F4/80, in the bone marrow, blood

and spleen: Ly6C^{hi} classical monocytes, and Ly6C^{-} CD43^{+} non-classical monocytes, which expressed more CX3CR1 than the Ly6C^{hi} monocytes (Figures 2A and S4A–B). Consistent with the previously established roles of IRF8 in monocyte differentiation (reviewed in (Yanez and Goodridge, 2016)) and Nur77 in classical to non-classical monocyte conversion (Hanna et al., 2011), we observed very few Ly6C^{hi} or Ly6C^{-} CD43^{+} monocytes in *Irf8*-deficient mice (Figures 2B and S4C), and Ly6C^{-} CD43^{+} monocytes (but not Ly6C^{hi} monocytes) were completely absent in mice lacking Nur77 (Figure 2C).

We next assessed production of the classical and non-classical monocytes by the GMP, MDP and mixed MP+cMoP fractions upon adoptive transfer into non-irradiated recipients. All three progenitor fractions yielded both Ly6C^{hi} and Ly6C^{-} CD43^{+} monocytes in an IRF8-dependent manner (Figures 2D and S4D), and Ly6C^{-} CD43^{+} monocyte production was Nur77-dependent (Figure 2E). Moreover, consistent with the production of non-classical monocytes by classical monocytes, all progenitors produced Ly6C^{hi} monocytes at earlier time points than Ly6C^{-} CD43^{+} monocytes (Figures 2D and S4D).

We also observed an additional subset of CD11b^{+} CD115^{+} Ly6G^{-} F4/80^{-} cells in the bone marrow and spleen (but not in the blood) that lacked both Ly6C and CD43 (Figure 2A). These Ly6C^{-} CD43^{-} cells strongly expressed CX3CR1 (Figure S4B), and were present at normal numbers in both *Irf8*-deficient and *Nur77 (Nr4a1)*-deficient mice (Figure 2B–C). In adoptive transfer experiments, they were produced by the MDP fraction in an IRF8- and Nur77-independent manner (Figure 2D–E). Notably however, neither GMPs nor the mixed MP+cMoP fraction yielded them (Figures 2D–E and S4D), which indicated that they are derived from MDPs, but arise independently of cMoPs.

Further characterization of the Ly6C^{-} CD43^{-} subset revealed that, in addition to CD11b and CD115, most of these cells in the bone marrow, and all of these cells in the spleen, strongly expressed CD11c, Zbtb46 (a transcription factor expressed only by cells of the cDC lineage; (Meredith et al., 2012; Satpathy et al., 2012)), MHC II and Flt3 (Figures 2F and S4E–F). This suggests that these cells are not monocytes, but instead belong to the cDC lineage. We considered whether exclusion of CD11c^{+} cells from the CD11b^{+} CD115^{+} gate is sufficient for reliable identification of the Ly6C^{-} monocytes. However, while this approach does remove the Ly6C^{-} CD43^{-} cells (data not shown), it is not a suitable alternative to CD43 staining for accurate evaluation of Ly6C^{-} monocytes, because some Ly6C^{-} CD43^{+} monocytes also express CD11c (Figure 2F), albeit to a lesser extent than DCs.

Taken together, our data indicate that the GMP and MDP pathways both yield classical Ly6C^{hi} monocytes (IRF8-dependent) and non-classical Ly6C^{-} monocytes (IRF8- and Nur77-dependent).

GMPs, MDPs and their progeny exhibit distinct gene expression signatures

We next addressed the possibility that although GMPs and MDPs both produced Ly6C^{hi} and Ly6C^{-} CD43^{+} monocytes, the limited number of surface markers used to define these monocyte subsets may not have revealed differences between the GMP- and MDP-derived monocytes. We therefore performed RNA sequencing to compare gene expression by the progeny (monocyte-committed progenitors and Ly6C^{hi} monocytes) of GMPs versus MDPs.

Since known markers do not enable us to distinguish between MPs and cMoPs, or between monocytes derived from GMPs and MDPs, we instead derived these cells from GMPs and MDPs *in vitro* using M-CSF. We established independent cultures of GMPs and MDPs (two replicate cultures each of GMPs and MDPs pooled from 20 mice), and isolated the monocyte-committed progenitors (MPs and cMoPs) and Ly6C^{hi} monocytes (GMP-derived and MDP-derived) that they produced (Figure S5A–B). We harvested and pooled cells produced over multiple days (e.g. Ly6C^{hi} monocytes in GMP cultures on days 2, 3 and 4) to negate gene expression differences between immature and mature cells. We performed bulk RNA sequencing of these cells (MPs, cMoPs, and GMP- and MDP-derived Ly6C^{hi} monocytes), as well as the *ex vivo* GMP and MDP fractions from which they were derived.

Principal Component Analysis (PCA) revealed that the MPs and cMoPs were distinct cell types, and similarly that the GMP-derived Ly6C^{hi} monocytes were distinct from their MDP-derived counterparts (Figure 3A). As expected for progenitors with distinct lineage potential, there was considerable variation between the GMPs and MDPs: 6.75% of all genes expressed by these progenitors (932 genes) were enriched in GMPs, and 2.95% (407 genes) were enriched in MDPs (Figure S5C). Comparison of the monocyte-committed progenitors derived from them also revealed notable differences in gene expression: the majority of genes were similarly expressed in MPs and cMoPs, but 2.03% of all genes expressed by these progenitors (270 genes) were enriched in MPs, and 1.63% (216 genes) in cMoPs (Figure 3B). Similarly, 0.97% of Ly6C^{hi} monocyte genes (129 genes) were enriched in GMP-derived Ly6C^{hi} monocytes, and 1.81% (240 genes) in MDP-derived Ly6C^{hi} monocytes (Figure 3B).

Many of the genes enriched in the GMP- and MDP-derived monocytes were also enriched in their respective progenitors (GMPs and MPs, or MDPs and cMoPs) (Figures 3C and S5D). Indeed, 36 genes were enriched at all three stages of the GMP pathway, and 44 genes were enriched at all stages of the MDP pathway (Figure S5D). In contrast, there was very little overlap of enriched genes between cells of the GMP and MDP pathways (Figures 3C and S5D).

We next compared gene expression by the progenitors (GMPs, MDPs, MPs and cMoPs) with the gene signatures of progenitor populations recently identified by single-cell RNA sequencing of hematopoietic progenitors (Olsson et al., 2016). Analysis revealed that the GMPs and MDPs expressed genes associated with HSCs and early progenitors (HSCP and MPP) as well as genes that are characteristic of megakaryocyte and erythrocyte progenitors (Figure S6A), even though GMPs and MDPs did not produce megakaryocytes and erythrocytes (Figure S2B). Following differentiation to MPs and cMoPs, these gene modules were lost (Figure S6A). The GMPs also expressed some genes associated with myeloid and granulocyte progenitors, and these signatures were more pronounced in the MPs (Figure S6A). In contrast, both the MDPs and cMoPs expressed monocyte and DC progenitor signatures (Figure S6A).

We also probed this single-cell bone marrow progenitor dataset to investigate whether we could detect MPs and cMoPs among the endogenous monocyte progenitors. Clustering of the monocyte progenitors using the MP and cMoP gene signatures identified in bulk

sequencing revealed two major subsets, corresponding to MPs and cMoPs (Figures 3D and S6B). These monocyte progenitor subsets were also evident as sub-clusters within the previously reported panorama of bone marrow progenitors (Figure 3E; (Olsson et al., 2016)). Thus the *in vitro* cultures reliably recapitulated *in vivo* monocyte progenitor differentiation, and supported our revised myelopoiesis model of 2 independent pathways of monocyte production.

GMPs produce "neutrophil-like" Ly6C^{hi} monocytes

We next examined the gene expression differences between the GMP- and MDP-derived Ly6C^{hi} monocytes in relation to immune cell gene expression profiles in the Immunological Genome Project (ImmGen) database. We found that the genes enriched in GMP-derived Ly6C^{hi} monocytes were more highly expressed by neutrophils (and to a lesser extent macrophages) than other immune cell types (Figure 4A), while the genes enriched in MDP-derived Ly6C^{hi} monocytes showed slightly higher expression among macrophages and DCs (Figure 4B).

We hypothesized that differential expression of myeloid transcription factors by the progenitors might account for these relationships. The master myeloid regulators *Spi1* (encodes PU.1) and *Cebpa* (c/EBPα) were highly expressed in GMPs and MPs, as well as MDPs and cMoPs (Figure 4C). In contrast, GMPs strongly expressed the neutrophil transcription factors *Gfi1* and *Cebpe* (c/EBPε), and MDPs strongly expressed the monocyte and DC transcription factors *Irf8* and *Klf4* (Figure 4C). Upon commitment to monocyte production, MPs upregulated *Irf8* and *Klf4*, but also maintained higher *Gfi1* expression than cMoPs (Figure 4C). Thus, *Gfi1* expression by the monocyte-committed progenitors reflected their origins i.e. GMP-derived MPs and MDP-derived cMoPs exhibited high and intermediate *Gfi1* expression respectively. These data suggest that differential patterns of transcription factor expression by the progenitors account for the relationship of GMP- and MDP-derived Ly6C^{hi} monocytes to neutrophils versus macrophages and DCs respectively.

We also used a double-reporter mouse (see Experimental Procedures) to assess expression of the IRF8 and Gfi1 transcription factors, which specify monocyte and neutrophil fate respectively. Consistent with our previous studies (Olsson et al., 2016; Yanez et al., 2015) and the RNA sequencing data, IRF8-GFP was barely detectable in *ex vivo* GMPs, but strongly expressed by MPs derived from them in M-CSF cultures, whereas e*x vivo* MDPs and the cMoPs derived from them both strongly expressed IRF8-GFP (Figure 4D). In contrast, Gfi1-tdTomato expression was strongest in the MPs (Figure 4D).

Taken together, the data suggested that the neutrophil-like transcription factor profile of the GMPs and MPs may shape the function of the monocytes they produce. Consistent with this hypothesis, we noticed that a number of granule genes typically expressed by neutrophils, in particular the primary granule proteases neutrophil elastase (*Elane*), proteinase 3 (*Prtn3*), and cathepsin G (*Ctsg*), were more strongly expressed by GMP-derived Ly6C^{hi} monocytes than MDP-derived Ly6C^{hi} monocytes (Figure 5A). The transcript encoding Serpinb1a, an inhibitor of ELANE, PRTN3 and CTSG activity, was also enriched in the GMP-derived Ly6C^{hi} monocytes (Figure 5A).

In vivo validation of the relationship between GMP-derived Ly6C^{hi} monocytes and neutrophils also revealed larger amounts of myeloperoxidase (MPO) protein in Ly6C^{hi} monocytes derived from adoptively transferred GMPs than in Ly6C^{hi} monocytes derived from MDPs (Figure 5B). The GMP-derived Ly6C^{hi} monocytes possessed similar amounts of MPO to neutrophils in the bone marrow, and slightly less MPO than neutrophils in the spleen (Figure 5B). We also noticed that the two monocyte subsets were morphologically distinct. The *in vivo* GMP-derived Ly6C^{hi} monocytes were larger (higher forward scatter) and more granular (higher side scatter) than the MDP-derived Ly6C^{hi} monocytes when assessed by flow cytometry (Figure 5B), and we confirmed their larger size by microscopy (Figure 5C). Importantly, despite their size and granularity, the GMP-derived Ly6C^{hi} monocytes exhibited a mononuclear morphology and thus resembled monocytes and macrophages rather than neutrophils (Figure 5C). Taken together, our data therefore indicated that GMPs produce Ly6C^{hi} monocytes with “neutrophil-like” characteristics.

MDPs yield monocyte-derived DC (moDC)-producing Ly6C^{hi} monocytes

We also noticed that MDP-derived Ly6C^{hi} monocytes expressed more CD11c on average than their counterparts in the GMP pathway, and slightly more MHCII (Figure S7A). This was consistent with their relationship to DCs (Figure 4B), although both CD11c and MHCII were much less strongly expressed by these monocytes than by splenic cDCs (Figure S7A). We therefore next assessed the ability of the two pathways to produce macrophages and monocyte-derived DCs (moDCs). Both pathways yielded macrophages in *in vitro* cultures with M-CSF (Figure 5D–F) and *in vivo* following adoptive transfer of GMPs and MDPs (not shown), but only the MDP pathway yielded moDCs in GM-CSF cultures (Figure 5G–I). Importantly, we confirmed that moDCs (CD11c^{+} MHCII^{hi} cells that were also CD86^{hi} and F4/80^{lo}) were specifically produced by MDP- and not GMP-derived Ly6C^{hi} monocytes (Figures 5I and S7B–C). We also noticed that CD11c^{+} MHC$^{–/lo}$ cells produced by MDP-derived Ly6C^{hi} monocytes in GM-CSF cultures expressed more CD86 than CD11c^{+} MHC$^{–/lo}$ cells produced by GMP-derived Ly6C^{hi} monocytes (Figure S7B–C).

A recent report demonstrated that moDCs originate from a subset of Ly6C^{hi} monocytes expressing the genes encoding MHCII, Flt3 and CD209a (Menezes et al., 2016). Consistent with this, we observed much stronger expression of these genes by MDP-derived Ly6C^{hi} monocytes than their GMP-derived counterparts (Figure 5J). Taken together, our data therefore demonstrate that moDCs arise exclusively from MDP-derived Ly6C^{hi} monocytes.

Single-cell RNA sequencing confirms the existence of “neutrophil-like” and moDC-producing subsets among bone marrow Ly6C^{hi} monocytes

To evaluate endogenous monocyte heterogeneity, and in particular to determine the proportion of “neutrophil-like” monocytes, we next performed single-cell RNA sequencing of Ly6C^{hi} monocytes from the bone marrow. We also profiled a subset of Ly6C^{hi} monocytes from the IRF8-GFP Gfi1-tdTomato reporter mouse that strongly expressed both reporter proteins (IRF8-GFP^{hi} Gfi1-tdTomato^{hi}; Figures 6A and S7D), and were larger and more granular than other Ly6C^{hi} monocytes (Figure 6A–B). Analysis of the GMP- and MDP-derived Ly6C^{hi} monocyte signature genes identified by bulk RNA sequencing (G-mono^{UP} and M-mono^{UP} genes; Figure 3B) using both AltAnalyze (Olsson et al., 2016) and Cytobank

(Kotecha et al., 2010) revealed a subset of Ly6C^{hi} monocytes that were enriched for GMP-derived Ly6C^{hi} monocyte signature genes, including neutrophil granule protein genes (Figure 6C–F). The IRF8-GFP^{hi} Gfi1-tdTomato^{hi} Ly6C^{hi} monocytes clustered with these "neutrophil-like" monocytes (Figure 6C–F), which comprised ~12% of the total Ly6C^{hi} monocytes. These "neutrophil-like" Ly6C^{hi} monocytes were also revealed using unsupervised clustering (Figure S7E).

Both the "neutrophil-like" monocyte cluster and the IRF8-GFP^{hi} Gfi1-tdTomato^{hi} Ly6C^{hi} monocytes strongly expressed *Irf8* mRNA, but lacked detectable *Gfi1* mRNA (Figure S7F), despite the continued presence of the tdTomato protein in the reporter cells (Figure 6A). The apparent protein expression may therefore reflect the longer half-life of the fluorescent protein compared to the transcription of the *Gfi1* gene (Olsson et al., 2016). This would suggest that the neutrophil-like gene signature was programmed in the MPs that produced these monocytes, which did express detectable *Gfi1* mRNA (Figure S7F). Alternatively, a previous report described Gfi1 protein accumulation in human monocytes despite low mRNA, due to reduced proteasomal degradation of Gfi1 (Marteijn et al., 2007). Thus Gfi1 protein may still have been present in the GMP-derived Ly6C^{hi} monocytes, even after *Gfi1* transcription ceased.

In addition to the "neutrophil-like" monocytes, we also detected a smaller, separate subset of Ly6C^{hi} monocytes expressing *Cd209a*, *H2-Ab1*, *H2-Aa* and *Flt3* (Figure S7G), which corresponded to the recently described moDC-producing monocytes (Menezes et al., 2016). Importantly, expression of the cDC transcription factor *Zbtb46* was not detected in any of the Ly6C^{hi} monocytes (Figure S7G). Thus, single-cell transcriptomic profiling demonstrated that the GMP- and MDP-derived Ly6C^{hi} monocyte subsets predicted by our *in vitro* and *in vivo* differentiation analyses existed among endogenous bone marrow monocytes.

GMP- and MDP-derived Ly6C^{hi} monocytes are produced in response to different microbial stimuli

Finally, we hypothesized that, in addition to yielding monocytes with different gene expression profiles, GMPs and MDPs may be separately mobilized to produce monocytes under distinct conditions, such as in response to different pathogens. Infection induces a pathogen-specific emergency myelopoiesis response that is characterized by the production of different combinations of myeloid cell subsets (Basu et al., 2000; Serbina et al., 2009; Yanez et al., 2011). Thus, microbial components or host factors produced in response to them may differentially mobilize GMPs and MDPs to produce monocytes.

Consistent with this hypothesis, we noticed that two diverse microbial components induced different emergency myelopoiesis responses. Lipopolysaccharide (LPS) preferentially stimulated neutrophil and monocyte production (Figure 7A) after initially depleting neutrophil numbers in the bone marrow (due to recruitment into the periphery). In contrast, upon intracellular delivery by co-administration with DOTAP, unmethylated CpG DNA specifically induced monocyte and cDC production (Figure 7A).

We therefore examined the ability of LPS and CpG to promote the *in vivo* differentiation of adoptively transferred GMPs and MDPs. LPS injection increased the yield of GMP-derived

Ly6C^{hi} monocytes, while CpG injection had no effect on GMP differentiation (Figure 7B). In contrast, the yield of MDP-derived Ly6C^{hi} monocytes increased following injection of CpG, but not LPS (Figure 7B). GMPs also produced elevated numbers of neutrophils in response to LPS (but not CpG) injection, and MDPs yielded more DCs in response to CpG (but not LPS) injection (Figure 7B). Consistent with their lineage potential under steady-state conditions, GMPs did not give rise to DCs, and MDPs did not produce neutrophils, under these emergency conditions (Figure 7B).

Moreover, following LPS, but not CpG, injection into IRF8-GFP Gfi1-tdTomato reporter mice, we observed proportionately more IRF8-GFP^{hi} Gfi1-tdTomato^{hi} Ly6C^{hi} monocytes in the bone marrow (Figure 7C), consistent with specific targeting of the GMP pathway to promote the production of “neutrophil-like” monocytes. Thus, the existence of two independent pathways of monocyte differentiation permits the production of specific combinations of myeloid cell subsets under distinct circumstances via differential targeting of GMPs and MDPs.

Discussion

Our study has revealed two independent pathways of monocyte differentiation from bone marrow progenitors. Both pathways originate in the CMP-Flt3^{+} CD115^{lo} fraction, although it is not currently clear whether they are derived from a single parental cell or two distinct progenitors that share the surface markers used to define that fraction. GMP differentiation then proceeds via a CMP-Flt3^{-} progenitor, while MDP differentiation does not. GMPs specifically defined as cells with the potential to produce both granulocytes (neutrophils) and monocytes have been convincingly demonstrated in previous studies (especially in colony-forming assays; (Akashi et al., 2000; Yanez et al., 2015)). In contrast, the existence of bipotent or oligopotent MDPs with the ability to yield both monocytes and DCs is more controversial (Sathe et al., 2014), and it is possible that the MDP fraction may comprise a mixture of progenitors committed to either monocyte or DC production. Nevertheless, our data collectively demonstrate that both the GMP and MDP fractions yield monocytes, and they do so independently.

A recent paper describing human monocyte-committed progenitors cast doubt on the presumed hierarchical relationship between human GMPs and MDPs, because GMPs failed to produce DCs in *in vitro* assays (Kawamura et al., 2017). Thus the two separate pathways of monocyte production by GMPs and MDPs that we have demonstrated in mice likely also exist in humans.

Our comparison of the gene expression profiles of the progenitors with the gene signatures of cell states recently identified by single-cell RNA sequencing (Olsson et al., 2016) supports the existence of the two pathways of monocyte differentiation. It is interesting to note that despite not possessing megakaryocyte or erythrocyte potential, the GMPs and MDPs exhibited megakaryocyte and erythrocyte gene signatures, which were subsequently lost as they differentiated. This observation supports the development of both GMPs and MDPs from progenitors that do possess megakaryocyte and erythrocyte potential. Similarly, our transcriptomic analyses demonstrated that MPs and cMoPs retained granulocyte and DC

signatures respectively, even though they had already committed to monocyte production, and suggested that these gene signatures shape the function of at least some of their progeny.

We have shown that the GMP and MDP pathways both yield Ly6C^{hi} and Ly6C^{-} CD43^{+} monocytes, and that Ly6C^{-} CD43^{+} monocyte (as well as Ly6C^{hi} monocyte) production is IRF8-dependent. Although we have not directly demonstrated a hierarchical relationship in this study, our data support the previously reported model of Ly6C^{-} monocyte production by Ly6C^{hi} monocytes (Hanna et al., 2011; Yona et al., 2013). This model has been challenged by the demonstration that although *Irf8*-deficient mice lack Ly6C^{hi} monocytes, they do possess some CD11b^{+} CD115^{+} Ly6C^{-} cells (Kurotaki et al., 2013). We have demonstrated that some CD11b^{+} CD115^{+} Ly6C^{-} cells in the spleen and bone marrow (Ly6C^{-} CD43^{-} cells) are derived from MDPs but not cMoPs, and that these cells are produced in an IRF8- and Nur77-independent manner and more closely resemble cDCs than monocytes. These observations highlight the importance of defining monocyte subsets using CD43 as well as Ly6C, and may reconcile apparent differences reported in previous studies.

Our data demonstrated two potential reasons for the existence of two independent pathways of monocyte production. Firstly, the two pathways appear to yield functionally distinct monocyte subsets. Along with another recent report (Menezes et al., 2016), our single-cell RNA sequencing analysis revealed considerable heterogeneity among murine classical (Ly6C^{hi} monocytes), and human classical monocytes appear to be similarly heterogeneous (Villani et al., 2017). Our other analyses demonstrated differential production of classical monocyte subsets by GMPs and MDPs. The “neutrophil-like” monocytes produced by GMPs expressed several granule enzymes, including similar amounts of MPO to neutrophils, which suggests that they may be better equipped for direct pathogen killing. We also demonstrated that moDCs are specifically produced by the MDP pathway. Thus the GMP and MDP pathways produce classical monocyte subsets that are functionally related to their neutrophil and DC “cousins” respectively. The origins of other Ly6C^{hi} monocyte subsets revealed by single-cell RNA sequencing remain to be determined.

Importantly, the “neutrophil-like” Ly6C^{hi} monocytes, which we detected under steady-state conditions, appear to be distinct from the recently described fibrosis-inducing segregated-nucleus-containing atypical monocytes (SatM) produced following bleomycin treatment, which were Ly6C^{-}, had bi-lobed segmented nuclei and granulocyte characteristics, and were produced by GMPs but not by the mixed MP+cMoP fraction (Satoh et al., 2017).

A second potential reason for the existence of two pathways of monocyte production is that the relative contributions of GMPs and MDPs to the steady-state and emergency monocyte pools may differ. For instance, GMP- and MDP-derived monocytes might populate distinct tissues, or yield monocytes in different proportions in the spleen and bone marrow. Most DC production occurs in the spleen (a site of extramedullary hematopoiesis), so MDPs may be more active there. Our data also suggested that the two pathways may be mobilized to combat different types of pathogens, depending on the microbial components to which the immune system is exposed. The specific promotion of GMP differentiation by the bacterial cell wall component LPS, and MDP differentiation following intracellular sensing of CpG

DNA, supports this hypothesis and is consistent with the differential emergency myelopoiesis responses induced by these two microbial components.

The progenitors may be mobilized following direct detection of the microbial components, or in response to cytokines or other host factors produced following microbial detection by differentiated hematopoietic or non-hematopoietic cells. We anticipate that progenitor mobilization is related to the type of immune response required for pathogen clearance. For instance, the GMP pathway may be activated in response to infections that require large numbers of neutrophils and monocytes to engulf and kill extracellular bacteria. In future studies, it will also be important to determine whether emergency myelopoiesis simply yields larger numbers of the same monocyte subsets produced in the steady-state, and/or distinct populations of “emergency monocytes”.

Finally, recent studies have demonstrated that monocyte and macrophage function can be modified for extended periods following microbial exposure due to metabolic and epigenetic changes (“trained immunity” or “innate immune memory”), which can confer long-term, lymphocyte-independent protection against pathogens and may underlie some clinical observations of heterologous effects of vaccination, especially in infants (Goodridge et al., 2016). These effects are likely maintained by epigenetic modification of myeloid progenitors (and even HSCs), as well as long-lived tissue-resident macrophages. Alterations in the repertoire of functionally distinct monocyte subsets produced by GMPs and MDPs may also underlie some observations of innate immune memory, and could impact monocyte production and function for extended periods.

STAR Methods Text

Contact for Reagent and Resource Sharing

Further information and requests for resources and reagents should be directed to and will be fulfilled by the Lead Contact, Helen Goodridge (Helen.Goodridge@csmc.edu).

Experimental Model and Subject Details

Mice—Wild-type C57BL/6 mice (CD45.2), congenic wild-type CD45.1 mice (B6.SJL-*Ptprc*^{a} *Pepc*^{b}/BoyJ), *Irf8*-deficient mice (B6(Cg)-*Irf8*$^{tm1.2Hm}$/J), *Nur77 (Nr4a1)*-deficient mice (B6;129S2-*Nr4a1*^{tm1Jmi}/J), CX3CR1-GFP reporter mice (B6.129P-*Cx3cr1*^{tm1Litt}/J) and Zbtb46-GFP reporter mice (129S-*Zbtb46*^{tm1Kmm}/J) were purchased from The Jackson Laboratories and maintained at either Cedars-Sinai Medical Center or Cincinnati Children’s Hospital Medical Center. Gfi1-Tomato IRF8-GFP dual reporter mice were bred at Cincinnati Children’s Hospital Medical Center by crossing Gfi1:H2B-tdTomato reporter mice (from Georges Lacaud, Cancer Research UK Manchester Institute, University of Manchester, UK; (Thambyrajah et al., 2016)) and IRF8-EGFP fusion protein reporter mice (from Herbert Morse III, National Institute of Allergy and Infectious Diseases, National Institutes of Health, USA; (Wang et al., 2014)). Female and male mice aged 6–10 weeks were used. All procedures were performed with IACUC approval.

Method Details

Cell staining for flow cytometry and FACS sorting—Fluorophore-conjugated antibodies used for flow cytometric analysis and FACS sorting were: CD34 (clone RAM34), FcγR (CD16 and CD32; clone 93) from eBioscience; Sca-1 (clone 108113), c-Kit (CD117; clone 2B8), Ly6C (clone HK1.4), Ly6G (clone 1A8), F4/80 (clone BM8), CD115 (clone AFS98), CD317 (clone 927), CD11c (clone N418), CD86 (clone GL-1), B220 (clone RA3-6B2), I-Ab (clone AF6-120.1), CD8α (clone 53-6.7), CD45.1 (clone A20), CD45.2 (clone 104) from BioLegend; CD43 (clone S7), CD11b (clone M1/70), CD135 (clone A2F10.1) from BD Biosciences; CCR2 (clone 475301) from R&D Systems. A cell fixation and permeabilization kit (BD Biosciences), a polyclonal anti-mouse MPO antibody (R&D Systems), and a secondary antibody (donkey anti-goat IgG, Abcam) were used for intracellular staining of MPO. Where possible, non-specific antibody binding was prevented by prior incubation with Fc block (anti-CD16 and anti-CD32). Fc blocking was not possible for identification of progenitors by FcγR expression so cells were stained for FcγR prior to staining with other antibodies. An LSRFortessa (BD Biosciences) was used for flow cytometry and data were analyzed with FlowJo.

Isolation of mouse bone marrow progenitors—Mouse progenitors were isolated from bone marrow (femurs and tibias) by a combination of magnetic and fluorescence sorting. Lineage marker negative cells (Lin^-) were first separated using a MACS lineage cell depletion kit (containing antibodies against CD5, CD11b, Gr-1, 7–4, and Ter-119) and an autoMACS Separator (both from Miltenyi). Lin^- cells were further fractionated using a FACS Aria III cell sorter (BD Biosciences) to isolate progenitor subpopulations as outlined in the text and figure legends.

***In vivo* progenitor differentiation—**Wild type CD45.2 progenitors were intravenously injected (25–50 × 10^3 cells/mouse in 100 μL PBS) into non-irradiated CD45.1 recipient mice on day 0. Mice were sacrificed at the indicated time points; bone marrow (femurs and tibias) and spleens were harvested and single cell suspensions were prepared. Erythrocytes were lysed with ammonium chloride and cells were MACS sorted (CD45.1 depletion) prior to flow cytometric analysis to enrich for $CD45.2^+$ donor-derived cells. Cells were stained for CD45.1, CD45.2, CD11b, Ly6C, Ly6G, F4/80, CD115, CD43, CCR2, mPDCA1 and CD11c for neutrophil, monocyte and dendritic cell identification, and CD45.1, CD45.2, CD11b, c-Kit, FcγR, CD34, Ly6C, CD115 and Flt3 for progenitor identification. Some mice were received an intravenous injection of either *Salmonella minnesota* LPS (25 μg/mouse; InvivoGen) or CpG (ODN1826, 5 μg/mouse; InvivoGen) + DOTAP (25 μg/mouse; Roche) two hours after progenitor transfer.

Colony-forming assays—To evaluate the myeloid and erythroid lineage potential of hematopoietic progenitors, 1 × 10^3 cells were plated in triplicate in MethoCult GFM3434 (STEMCELL Technologies; components include insulin, transferrin, stem cell factor, IL-3, IL-6, erythropoietin). Colonies were identified and counted 7 days later.

May-Grunwald Giemsa staining—GMPs and MDPs were labeled with CFSE (Life Technologies) prior to adoptive transfer into recipient mice. Donor-derived $Ly6C^{hi}$

monocytes (CFSE^{+} CD11b^{+} Ly6G^{-} CD115^{+} Ly6C^{hi} cells) were FACS sorted from the bone marrow and spleens of recipient mice 3 days later. Cytospin preparations of sorted cells were stained with May-Grunwald Giemsa stain (American MasterTech) according to the manufacturer's instructions, and bright-field images of the cells were captured using an Olympus BX51WI microscope.

Bulk RNA sequencing—GMPs and MDPs were isolated from the pooled bone marrow of 20 mice and cultured *in vitro* in media (RPMI with 10% FCS and 1% penicillin-streptomycin) supplemented with M-CSF (50 ng/ml; Peprotech). On days 2, 3 and 4 of culture, cells were harvested and FACS sorted for monocyte progenitors (c-Kit^{+} CD11b^{-} Ly6G^{-} Ly6C^{+} CD115^{+}) and Ly6C^{hi} monocytes (c-Kit^{-} CD11b^{+} Ly6G^{-} CD115^{+} Ly6C^{hi} F4/80^{-}). Whole cell lysates of cells isolated at the three timepoints were pooled for each cell type, and RNA was extracted from using an RNeasy mini kit (Qiagen). RNA was also extracted from the ex vivo GMP and MDP fractions from which the monocyte progenitors and monocytes were derived, as well as the GP and mixed MP+cMoP fractions. The whole process was repeated using 20 additional mice to obtain a replicate set of samples. RNA samples were quantified on a bioanalyzer, and RNA sequencing was performed at the Clinical Microarray Core in the Department of Pathology and Laboratory Medicine at the David Geffen School of Medicine at UCLA. Each sample was subjected to library preparation with a KAPA kit (Kapa Biosystems) and multiplexed across 4 lanes to yield a mean of 32.9 million 75 bp single-end reads per sample (standard deviation 1.7 million reads). High-throughput sequencing was conducted on an Illumina NextSeq. Sequences in FASTQ format were aligned to the mouse genome version GRCm38 (mm10) using STARalign (Dobin et al., 2013) with the following parameters: reduce spurious junctions filter BySJout (parameter –outFilterType), maximum of 20 multiple alignments allowed (–outFilterMultimapNmax), a minimum overhang of 8 b.p. for unannotated junctions vs 1 b.p. for annotated (–alignSJoverhangMin and –alignSJDBoverhangMin), no mismatch filter, minimum intron length 20 b.p. (–alignIntronMin), and maximum intron length set to 1 M.b.p. (–alignIntronMax). The bulk RNA-sequencing dataset has been deposited in GEO: GSE88982.

Single-cell RNA sequencing—Ly6C^{hi} monocytes (CD11b^{+} Ly6G^{-} CD115^{+} F4/80^{-} Ly6C^{hi} cells) were isolated from the bone marrow of wild-type mice (pooled from 5 mice) and Gfi1-Tomato IRF8-GFP mice (pooled from 3 mice) by FACS sorting and individual cells were prepared using the C1 Single-Cell Auto Prep System (Fluidigm) as previously described (Olsson et al., 2016), with visual inspection to confirm the capture of individual cells. Cell lysis, reverse transcription, cDNA quantification and library preparation were performed as previously described (Olsson et al., 2016). Single-cell libraries were subjected to paired-end 75 bp RNA-sequencing on a HiSeq 2500 (Illumina Inc.). 96 scRNA-seq libraries were sequenced per HiSeq 2500 gel (~300 million bp per gel). The single-cell RNA-sequencing dataset has been deposited in GEO: GSE104478.

Quantification and Statistical Analysis

Statistical and gene expression analyses—Statistical analyses for progenitor differentiation studies were performed using Student's t-tests. For analysis of the bulk RNA-

sequencing data, differential expression gene analyses were carried out using the limma-voom analysis pipeline from R/Bioconductor (Law et al., 2014). Genes with at least 1 count per million (cpm) in at least 2 samples were included, and normalized with calcNormFactors (method="TMM"). Normalized cpm values were used for the PCA analysis. The lmFit() function was then used to fit the linear models, and contrasts.fit() was applied to estimate differences between groups of samples. Finally, the treat() function was used to compute the empirical Bayes moderated t-tests relative to a minimum fold-change threshold of 2 at FDR<0.05 to identify differentially expressed genes. Data for ImmGen comparisons were obtained from the Gene Expression Omnibus database (GEO accession GSE15907) and plotted with R using ggplot2. A Mann-Whitney U test with Holm correction was used to compare each cell type with the other cell types. Expression of progenitor population-specific genes and selected markers previously defined in a single-cell RNA sequencing study (Olsson et al., 2016) was also evaluated. Analysis of the single-cell RNA sequencing data (both the Ly6C^{hi} monocytes and the previously sequenced monocyte progenitors (Olsson et al., 2016)) was performed as previously described using the ICGS automated workflow in AltAnalyze (Olsson et al., 2016), and using Cytobank (Kotecha et al., 2010). Gene selection is indicated in the figure legends. Differentially expressed genes were defined as $p<0.05$ in empirical Bayes moderated t-tests and fold change >2.

Data and Software Availability

Data Resources—The accession numbers for the RNA sequencing data reported in this paper are Gene Expression Omnibus (GEO): GSE88982 and GSE104478.

Supplementary Material

Refer to Web version on PubMed Central for supplementary material.

Acknowledgments

This study was supported by funds from the Board of Governors Regenerative Medicine Institute at Cedars-Sinai Medical Center (to HSG), development funds from Cedars-Sinai Medical Center (to SC, DH and BB), a grant from the National Institutes of Health (R01HL122661 to HLG), a Careers in Immunology fellowship from the American Association of Immunologists (to AY and HSG), and a Scholar Award from the American Society of Hematology (to AY). We thank Dr. Ritchie Ho for helpful discussions.

References

Akashi K, Traver D, Miyamoto T, Weissman IL. A clonogenic common myeloid progenitor that gives rise to all myeloid lineages. Nature. 2000; 404:193–197. [PubMed: 10724173]

Amir el AD, Davis KL, Tadmor MD, Simonds EF, Levine JH, Bendall SC, Shenfeld DK, Krishnaswamy S, Nolan GP, Pe'er D. viSNE enables visualization of high dimensional single-cell data and reveals phenotypic heterogeneity of leukemia. Nat Biotechnol. 2013; 31:545–552. [PubMed: 23685480]

Auffray C, Fogg DK, Narni-Mancinelli E, Senechal B, Trouillet C, Saederup N, Leemput J, Bigot K, Campisi L, Abitbol M, et al. CX3CR1+ CD115+ CD135+ common macrophage/DC precursors and the role of CX3CR1 in their response to inflammation. J Exp Med. 2009; 206:595–606. [PubMed: 19273628]

Basu S, Hodgson G, Zhang HH, Katz M, Quilici C, Dunn AR. "Emergency" granulopoiesis in G-CSF-deficient mice in response to Candida albicans infection. Blood. 2000; 95:3725–3733. [PubMed: 10845903]

Carlin LM, Stamatiades EG, Auffray C, Hanna RN, Glover L, Vizcay-Barrena G, Hedrick CC, Cook HT, Diebold S, Geissmann F. Nr4a1-dependent Ly6C(low) monocytes monitor endothelial cells and orchestrate their disposal. Cell. 2013; 153:362–375. [PubMed: 23582326]

D'Amico A, Wu L. The early progenitors of mouse dendritic cells and plasmacytoid predendritic cells are within the bone marrow hemopoietic precursors expressing Flt3. J Exp Med. 2003; 198:293–303. [PubMed: 12874262]

Dobin A, Davis CA, Schlesinger F, Drenkow J, Zaleski C, Jha S, Batut P, Chaisson M, Gingeras TR. STAR: ultrafast universal RNA-seq aligner. Bioinformatics. 2013; 29:15–21. [PubMed: 23104886]

Drissen R, Buza-Vidas N, Woll P, Thongjuea S, Gambardella A, Giustacchini A, Mancini E, Zriwil A, Lutteropp M, Grover A, et al. Distinct myeloid progenitor-differentiation pathways identified through single-cell RNA sequencing. Nat Immunol. 2016; 17:666–676. [PubMed: 27043410]

Fogg DK, Sibon C, Miled C, Jung S, Aucouturier P, Littman DR, Cumano A, Geissmann F. A clonogenic bone marrow progenitor specific for macrophages and dendritic cells. Science. 2006; 311:83–87. [PubMed: 16322423]

Geissmann F, Jung S, Littman DR. Blood monocytes consist of two principal subsets with distinct migratory properties. Immunity. 2003; 19:71–82. [PubMed: 12871640]

Geissmann F, Mass E. A stratified myeloid system, the challenge of understanding macrophage diversity. Semin Immunol. 2015; 27:353–356. [PubMed: 27038773]

Goodridge HS, Ahmed SS, Curtis N, Kollmann TR, Levy O, Netea MG, Pollard AJ, van Crevel R, Wilson CB. Harnessing the beneficial heterologous effects of vaccination. Nat Rev Immunol. 2016; 16:392–400. [PubMed: 27157064]

Guo G, Luc S, Marco E, Lin TW, Peng C, Kerenyi MA, Beyaz S, Kim W, Xu J, Das PP, et al. Mapping cellular hierarchy by single-cell analysis of the cell surface repertoire. Cell Stem Cell. 2013; 13:492–505. [PubMed: 24035353]

Hanna RN, Carlin LM, Hubbeling HG, Nackiewicz D, Green AM, Punt JA, Geissmann F, Hedrick CC. The transcription factor NR4A1 (Nur77) controls bone marrow differentiation and the survival of Ly6C- monocytes. Nat Immunol. 2011; 12:778–785. [PubMed: 21725321]

Hashimoto D, Chow A, Noizat C, Teo P, Beasley MB, Leboeuf M, Becker CD, See P, Price J, Lucas D, et al. Tissue-resident macrophages self-maintain locally throughout adult life with minimal contribution from circulating monocytes. Immunity. 2013; 38:792–804. [PubMed: 23601688]

Hettinger J, Richards DM, Hansson J, Barra MM, Joschko AC, Krijgsveld J, Feuerer M. Origin of monocytes and macrophages in a committed progenitor. Nat Immunol. 2013; 14:821–830. [PubMed: 23812096]

Ingersoll MA, Spanbroek R, Lottaz C, Gautier EL, Frankenberger M, Hoffmann R, Lang R, Haniffa M, Collin M, Tacke F, et al. Comparison of gene expression profiles between human and mouse monocyte subsets. Blood. 2010; 115:e10–19. [PubMed: 19965649]

Kawamura S, Onai N, Miya F, Sato T, Tsunoda T, Kurabayashi K, Yotsumoto S, Kuroda S, Takenaka K, Akashi K, et al. Identification of a Human Clonogenic Progenitor with Strict Monocyte Differentiation Potential: A Counterpart of Mouse cMoPs. Immunity. 2017; 46:835–848 e834. [PubMed: 28514689]

Kotecha N, Krutzik PO, Irish JM. Web-based analysis and publication of flow cytometry experiments. Curr Protoc Cytom Chapter. 2010; 10 Unit10 17.

Kurotaki D, Osato N, Nishiyama A, Yamamoto M, Ban T, Sato H, Nakabayashi J, Umehara M, Miyake N, Matsumoto N, et al. Essential role of the IRF8-KLF4 transcription factor cascade in murine monocyte differentiation. Blood. 2013; 121:1839–1849. [PubMed: 23319570]

Law CW, Chen Y, Shi W, Smyth GK. voom: Precision weights unlock linear model analysis tools for RNA-seq read counts. Genome Biol. 2014; 15:R29. [PubMed: 24485249]

Manz MG, Boettcher S. Emergency granulopoiesis. Nat Rev Immunol. 2014; 14:302–314. [PubMed: 24751955]

Marteijn JA, van der Meer LT, Van Emst L, de Witte T, Jansen JH, van der Reijden BA. Diminished proteasomal degradation results in accumulation of Gfi1 protein in monocytes. Blood. 2007; 109:100–108. [PubMed: 16888099]

McGrath KE, Frame JM, Palis J. Early hematopoiesis and macrophage development. Semin Immunol. 2015; 27:379–387. [PubMed: 27021646]

Menezes S, Melandri D, Anselmi G, Perchet T, Loschko J, Dubrot J, Patel R, Gautier EL, Hugues S, Longhi MP, et al. The Heterogeneity of Ly6Chi Monocytes Controls Their Differentiation into iNOS+ Macrophages or Monocyte-Derived Dendritic Cells. Immunity. 2016; 45:1205–1218. [PubMed: 28002729]

Meredith MM, Liu K, Darrasse-Jeze G, Kamphorst AO, Schreiber HA, Guermonprez P, Idoyaga J, Cheong C, Yao KH, Niec RE, et al. Expression of the zinc finger transcription factor zDC (Zbtb46, Btbd4) defines the classical dendritic cell lineage. J Exp Med. 2012; 209:1153–1165. [PubMed: 22615130]

Notta F, Zandi S, Takayama N, Dobson S, Gan OI, Wilson G, Kaufmann KB, McLeod J, Laurenti E, Dunant CF, et al. Distinct routes of lineage development reshape the human blood hierarchy across ontogeny. Science. 2016; 351:aab2116. [PubMed: 26541609]

Olsson A, Venkatasubramanian M, Chaudhri VK, Aronow BJ, Salomonis N, Singh H, Grimes HL. Single-cell analysis of mixed-lineage states leading to a binary cell fate choice. Nature. 2016; 537:698–702. [PubMed: 27580035]

Onai N, Kurabayashi K, Hosoi-Amaike M, Toyama-Sorimachi N, Matsushima K, Inaba K, Ohteki T. A clonogenic progenitor with prominent plasmacytoid dendritic cell developmental potential. Immunity. 2013; 38:943–957. [PubMed: 23623382]

Passlick B, Flieger D, Ziegler-Heitbrock HW. Identification and characterization of a novel monocyte subpopulation in human peripheral blood. Blood. 1989; 74:2527–2534. [PubMed: 2478233]

Paul F, Arkin Y, Giladi A, Jaitin DA, Kenigsberg E, Keren-Shaul H, Winter D, Lara-Astiaso D, Gury M, Weiner A, et al. Transcriptional Heterogeneity and Lineage Commitment in Myeloid Progenitors. Cell. 2015; 163:1663–1677. [PubMed: 26627738]

Pronk CJ, Rossi DJ, Mansson R, Attema JL, Norddahl GL, Chan CK, Sigvardsson M, Weissman IL, Bryder D. Elucidation of the phenotypic, functional, and molecular topography of a myeloerythroid progenitor cell hierarchy. Cell Stem Cell. 2007; 1:428–442. [PubMed: 18371379]

Sathe P, Metcalf D, Vremec D, Naik SH, Langdon WY, Huntington ND, Wu L, Shortman K. Lymphoid tissue and plasmacytoid dendritic cells and macrophages do not share a common macrophage-dendritic cell-restricted progenitor. Immunity. 2014; 41:104–115. [PubMed: 25035955]

Satoh T, Nakagawa K, Sugihara F, Kuwahara R, Ashihara M, Yamane F, Minowa Y, Fukushima K, Ebina I, Yoshioka Y, et al. Identification of an atypical monocyte and committed progenitor involved in fibrosis. Nature. 2017; 541:96–101. [PubMed: 28002407]

Satpathy AT, Kc W, Albring JC, Edelson BT, Kretzer NM, Bhattacharya D, Murphy TL, Murphy KM. Zbtb46 expression distinguishes classical dendritic cells and their committed progenitors from other immune lineages. J Exp Med. 2012; 209:1135–1152. [PubMed: 22615127]

Schulz C, Gomez Perdiguero E, Chorro L, Szabo-Rogers H, Cagnard N, Kierdorf K, Prinz M, Wu B, Jacobsen SE, Pollard JW, et al. A lineage of myeloid cells independent of Myb and hematopoietic stem cells. Science. 2012; 336:86–90. [PubMed: 22442384]

Serbina NV, Hohl TM, Cherny M, Pamer EG. Selective expansion of the monocytic lineage directed by bacterial infection. J Immunol. 2009; 183:1900–1910. [PubMed: 19596996]

Thambyrajah R, Mazan M, Patel R, Moignard V, Stefanska M, Marinopoulou E, Li Y, Lancrin C, Clapes T, Moroy T, et al. GFI1 proteins orchestrate the emergence of haematopoietic stem cells through recruitment of LSD1. Nat Cell Biol. 2016; 18:21–32. [PubMed: 26619147]

Villani AC, Satija R, Reynolds G, Sarkizova S, Shekhar K, Fletcher J, Griesbeck M, Butler A, Zheng S, Lazo S, et al. Single-cell RNA-seq reveals new types of human blood dendritic cells, monocytes, and progenitors. Science. 2017; 356

Wang H, Yan M, Sun J, Jain S, Yoshimi R, Abolfath SM, Ozato K, Coleman WG Jr, Ng AP, Metcalf D, et al. A reporter mouse reveals lineage-specific and heterogeneous expression of IRF8 during lymphoid and myeloid cell differentiation. J Immunol. 2014; 193:1766–1777. [PubMed: 25024380]

Yanez A, Goodridge HS. Interferon regulatory factor 8 and the regulation of neutrophil, monocyte, and dendritic cell production. Curr Opin Hematol. 2016; 23:11–17. [PubMed: 26554887]

Yanez A, Goodridge HS, Gozalbo D, Gil ML. TLRs control hematopoiesis during infection. Eur J Immunol. 2013; 43:2526–2533. [PubMed: 24122753]

Yanez A, Megias J, O'Connor JE, Gozalbo D, Gil ML. Candida albicans induces selective development of macrophages and monocyte derived dendritic cells by a TLR2 dependent signalling. PLoS One. 2011; 6:e24761. [PubMed: 21935459]

Yanez A, Ng MY, Hassanzadeh-Kiabi N, Goodridge HS. IRF8 acts in lineage-committed rather than oligopotent progenitors to control neutrophil vs monocyte production. Blood. 2015; 125:1452–1459. [PubMed: 25597637]

Yona S, Kim KW, Wolf Y, Mildner A, Varol D, Breker M, Strauss-Ayali D, Viukov S, Guilliams M, Misharin A, et al. Fate mapping reveals origins and dynamics of monocytes and tissue macrophages under homeostasis. Immunity. 2013; 38:79–91. [PubMed: 23273845]

Zhu YP, Thomas GD, Hedrick CC. 2014 Jeffrey M. Hoeg Award Lecture: Transcriptional Control of Monocyte Development. Arterioscler Thromb Vasc Biol. 2016; 36:1722–1733. [PubMed: 27386937]

Highlights

1. GMPs and MDPs independently produce functionally distinct inflammatory monocytes.
2. GMPs produce “neutrophil-like” inflammatory monocytes.
3. MDPs produce monocyte-derived dendritic cells (moDCs).
4. Microbial stimuli differentially regulate monocyte production by GMPs and MDPs.

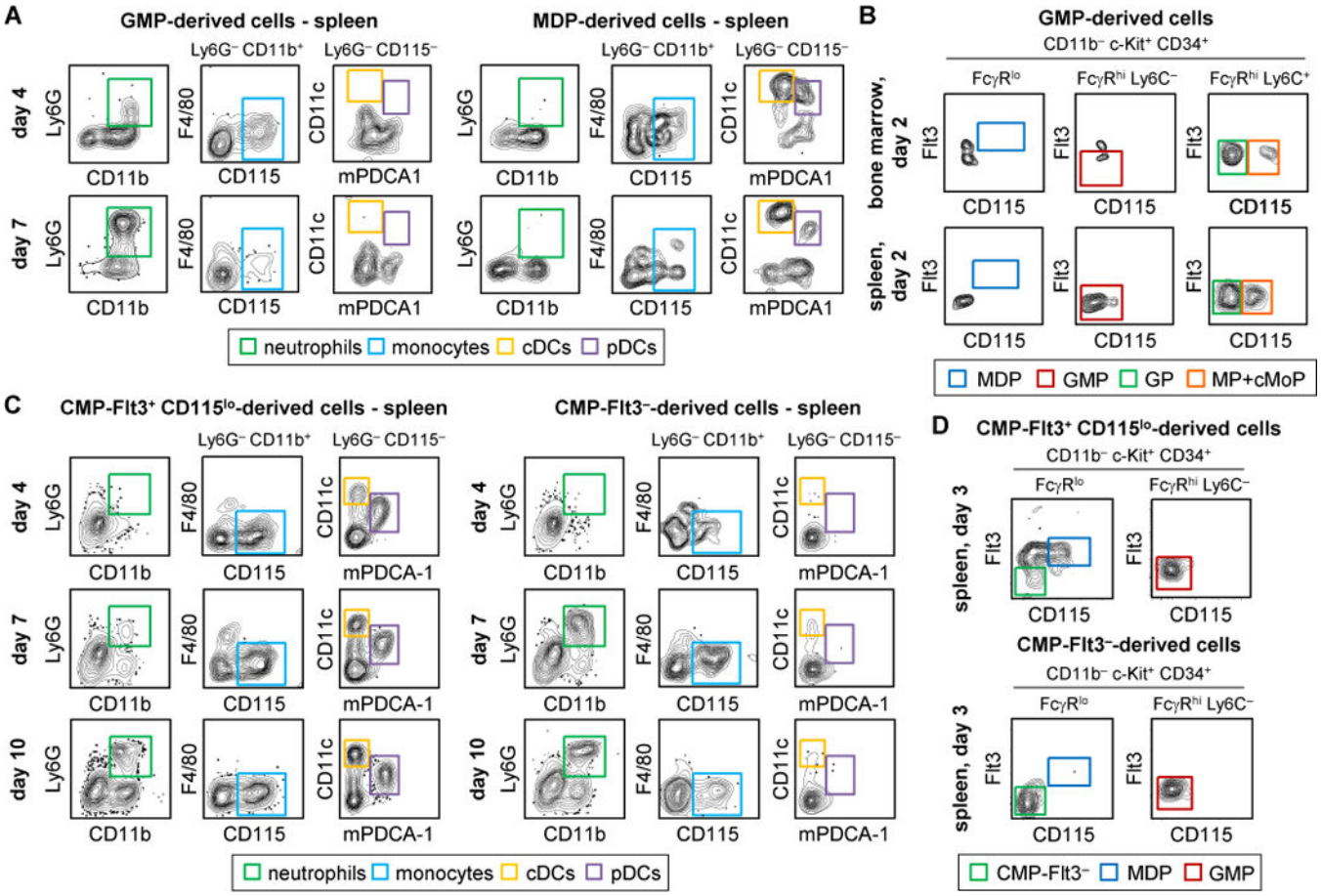

Figure 1. Independent production of monocytes by GMPs and MDPs

25,000–50,000 GMPs, MDPs, CMP-Flt3$^+$ CD115^{lo} or CMP-Flt3$^-$ progenitors isolated from CD45.2 donor mice (see Figure S1B) were injected i.v. into congenic CD45.1 recipient mice (non-irradiated) on day 0. Bone marrow and spleens were harvested from recipient mice at the indicated timepoints after progenitor injection, and single cell suspensions were enriched for CD45.2$^+$ (donor-derived) cells by MACS depletion of CD45.1$^+$ cells prior to staining to detect donor-derived progeny (CD45.2$^+$) by flow cytometry. Data presented in each panel are from one experiment that is representative of at least 3 independent experiments.

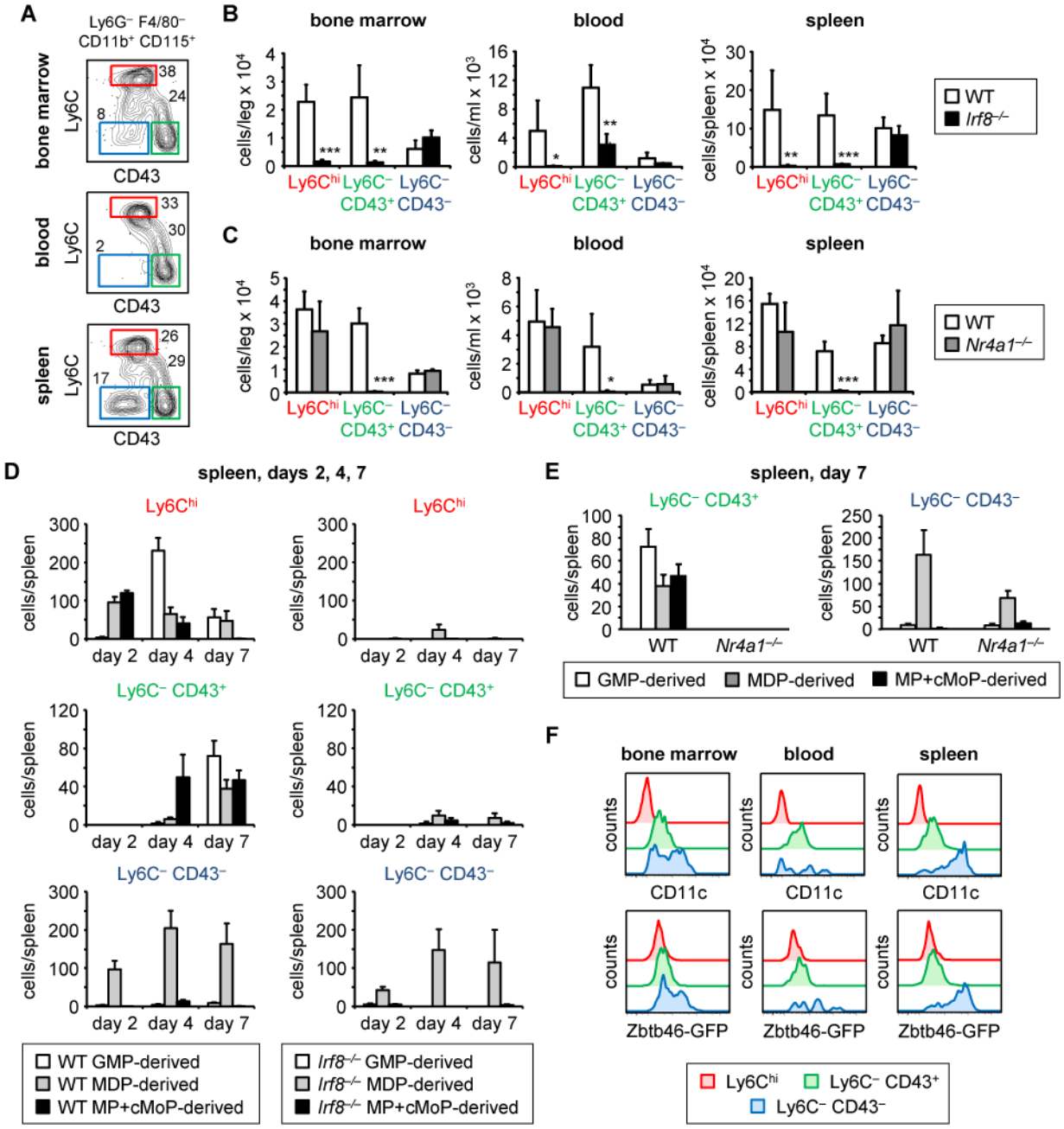

Figure 2. GMPs and MDPs produce both Ly6C^{hi} and Ly6C^{-} CD43^{+} monocytes

(A) To identify monocyte subsets in the bone marrow, blood and spleen of wild-type mice, Ly6C and CD43 expression by CD11b^{+} CD115^{+} Ly6G^{-} F4/80^{-} cells was assessed by flow cytometry (see Figure S4A for gating strategy). (B–C) Ly6C^{hi}, Ly6C^{-} CD43^{+} and Ly6C^{-} CD43^{-} subsets were assessed in the bone marrow, blood and spleen of wild-type (B–C), *Irf8*-deficient (B) and *Nur77 (Nr4a1)*-deficient (C) mice with additional gating of CCR2^{+} cells to identify Ly6C^{hi} monocytes due to the presence of incompletely differentiated Ly6C^{int} monoblasts in *Irf8*-deficient mice (Figure S4C and (Yanez et al., 2015)). Data are presented as mean plus standard deviation of 5 mice, and statistical significance was assessed by Student's t-test (*p<0.05, **p<0.01, ***p<0.001). (D–E) 25,000 GMPs, MDPs

or MPs+cMoPs isolated from wild-type (D–E), *Irf8*-deficient (D) or *Nur77 (Nr4a1)*-deficient (E) donor mice (all CD45.2) were injected i.v. into congenic CD45.1 recipient mice (non-irradiated) on day 0. Spleens were harvested from recipient mice at the indicated timepoints after progenitor injection, and splenocytes were enriched for $CD45.2^+$ (donor-derived) cells prior to assessment of donor-derived $Ly6C^{hi}$ (and $CCR2^+$), $Ly6C^-$ $CD43^+$ and $Ly6C^-$ $CD43^-$ cells by flow cytometry (see Figure S4D for gating strategy). Data are presented as mean plus standard error of 3–4 mice that received progenitors in independent experiments. (F) CD11c and Zbtb46 expression by $Ly6C^{hi}$, $Ly6C^-$ $CD43^+$ and $Ly6C^-$ $CD43^-$ cells in the bone marrow, blood and spleen of Zbtb46-GFP transgenic mice was assessed by flow cytometry.

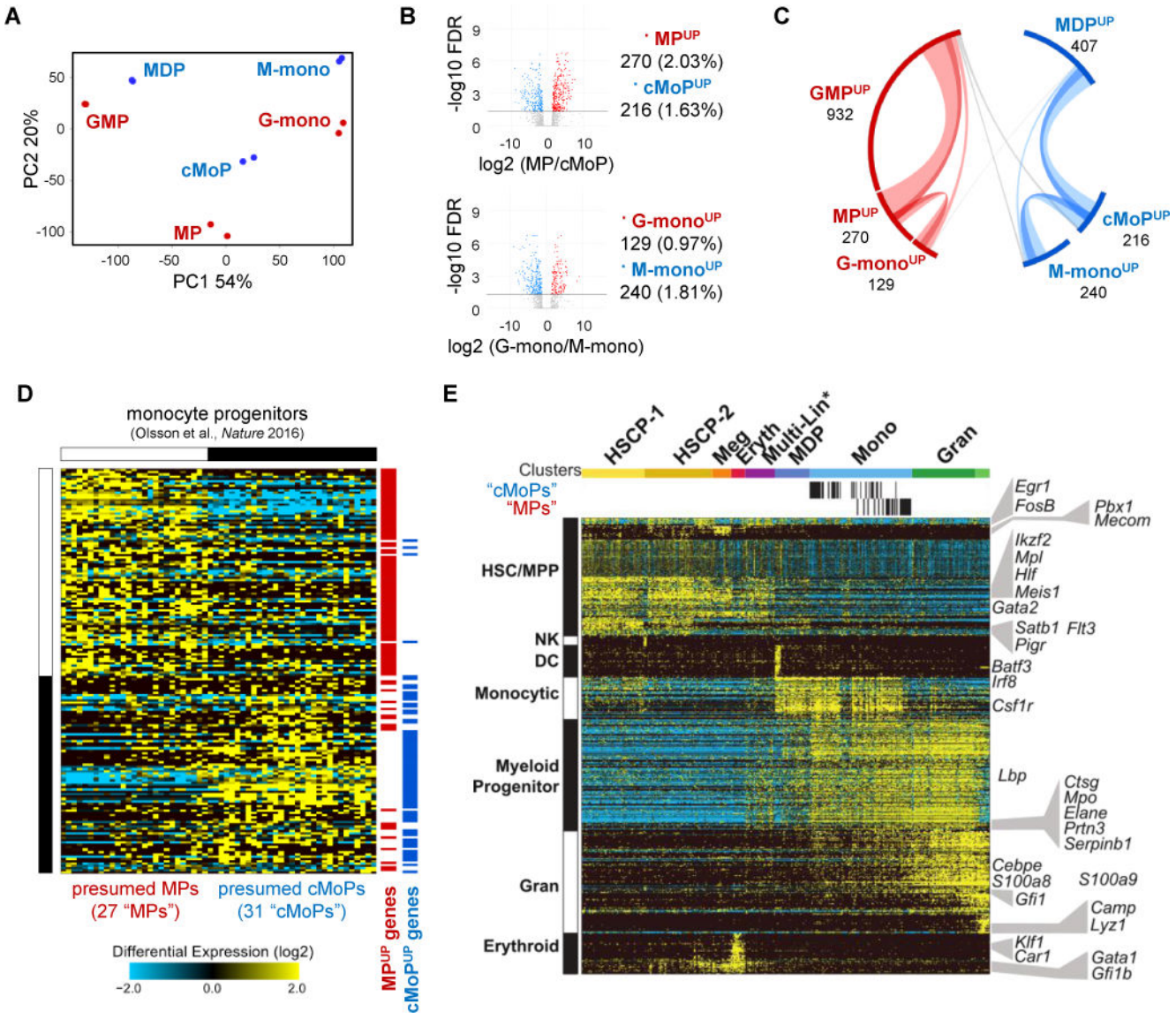

Figure 3. Transcriptomic profiling of GMP- and MDP-derived monocyte progenitors and Ly6C^{hi} monocytes

GMPs and MDPs were isolated from mouse bone marrow and cultured *in vitro* with M-CSF. Monocyte-committed progenitors (MPs or cMoPs) and Ly6C^{hi} monocytes were isolated from the cultures (see also Figure S5A–B), and RNA was isolated from these cells, as well as the GMPs and MDPs from which they were derived. Two replicate samples of each cell type were derived from independent cultures (each using GMPs or MDPs pooled from 20 mice) for RNA sequencing. (A) Principal component analysis of gene expression by the parental progenitors (GMPs and MDPs), monocyte-committed progenitors (MPs and cMoPs), and Ly6C^{hi} monocytes (GMP- and MDP-derived: G-mono and M-mono respectively). (B) Gene expression by the monocyte-committed progenitors and Ly6C^{hi} monocytes was compared between the two pathways. Volcano plots of differentially expressed genes (2-fold, adjusted p value < 0.05) are shown. The number of enriched (^{UP}) genes in each subset is noted at the side, and this is also displayed as a percentage of the

total genes expressed by each pair (e.g. number of MP-enriched (MP^{UP}) genes/total number of genes expressed by MPs and cMoPs). (C) Circos plot of the enriched genes for each subset in the two pathways. In the outer circle, genes enriched at the indicated stage of the GMP lineage (compared to its counterpart in the MDP lineage) are red, while those enriched at the indicated stage of the MDP lineage (compared to the GMP lineage) are blue. Lines linking the subsets indicate genes that are enriched in multiple subsets, with red and blue lines indicating conservation within the same pathway (GMP or MDP, respectively). Only genes that are differentially expressed in at least one of the cell types are shown. (D) Expression of MP^{UP} and $cMoP^{UP}$ genes (identified by bulk RNA sequencing; 2-fold, $p<0.05$) by 58 individual LKS^{-} $CD34^{+}$ $Fc\gamma R^{hi}$ mouse bone marrow cells previously identified as monocyte-committed progenitors by single-cell RNA sequencing (Olsson et al., 2016). Clustering was performed in AltAnalyze using HOPACH (correlation distance), permitting the identification of 2 subsets corresponding to presumed MPs and cMoPs ("MPs" and "cMoPs") as indicated. Red and blue tick marks indicate MP^{UP} and $cMoP^{UP}$ genes respectively (genes not detected by single-cell RNA sequencing are not shown). (E) Individual monocyte-committed progenitors from the LKS^{-} $CD34^{+}$ $Fc\gamma R^{hi}$ fraction of mouse bone marrow that were identified as presumed MPs or cMoPs ("MPs" or "cMoPs"; black tick marks) were viewed within the panorama of bone marrow progenitors profiled previously by single-cell RNA sequencing (Olsson et al., 2016). Cells sorted from other cell fractions (e.g. LKS^{-} $CD34^{+}$ $Fc\gamma R^{int}$ cells) and annotated as monocyte progenitors (Olsson et al., 2016) were not characterized.

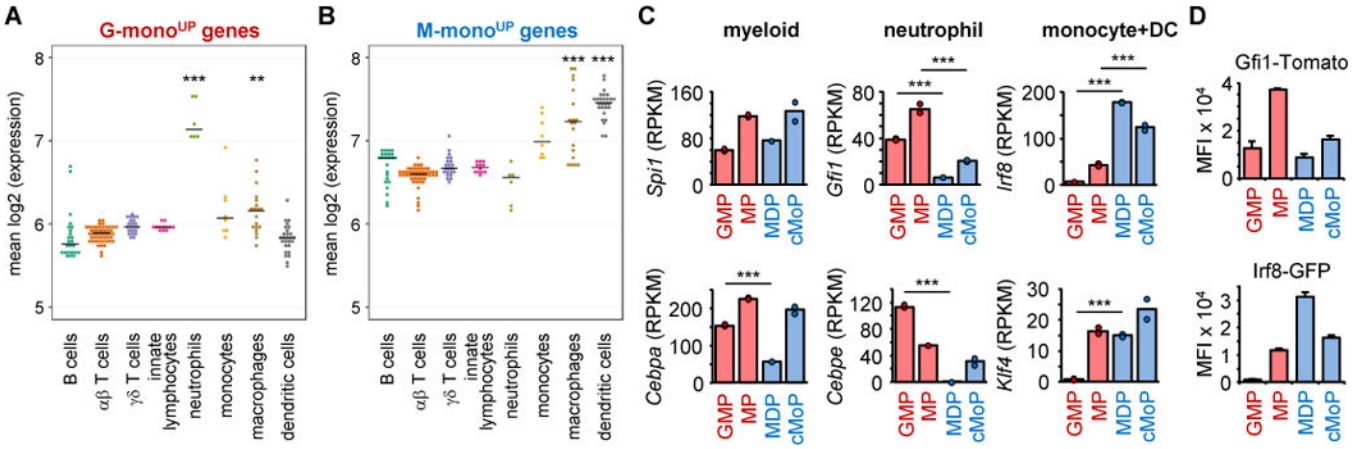

Figure 4. Relationship of GMP-derived and MDP-derived Ly6C^{hi} monocytes to other immune cells

(A–B) Expression of the enriched gene sets of GMP- and MDP-derived Ly6C^{hi} monocytes (A, 129 G-mono^{UP} genes; B, 240 M-mono^{UP} genes) by immune cells in the V1 dataset of the Immunological Genome Project (ImmGen) database. Each dot represents the mean expression of all G-mono^{UP} or M-mono^{UP} genes by an individual sample of the indicated cell type (6–49 samples per cell type, e.g. 6 neutrophil samples, 49 αβ T cell samples). Horizontal bars indicate median expression values for each cell type. Statistical significance was assessed using a Mann-Whitney U test with Holm correction to compare each cell type with the other cell types (**p<0.01, ***p<0.001). (C) Expression of myeloid, neutrophil and monocyte+DC transcription factors by the *ex vivo* GMPs and MDPs, and the MPs and cMoPs derived from them *in vitro*. Statistical significance was assessed using an empirical Bayes moderated t-test (***p<0.05). (D) Reporter protein expression by *ex vivo* GMPs and MDPs isolated from the bone marrow of Gfi1-Tomato IRF8-GFP transgenic mice, and MPs and cMoPs derived from them *in vitro*. Data are presented as mean plus standard deviation of MFIs from 3 independent cultures.

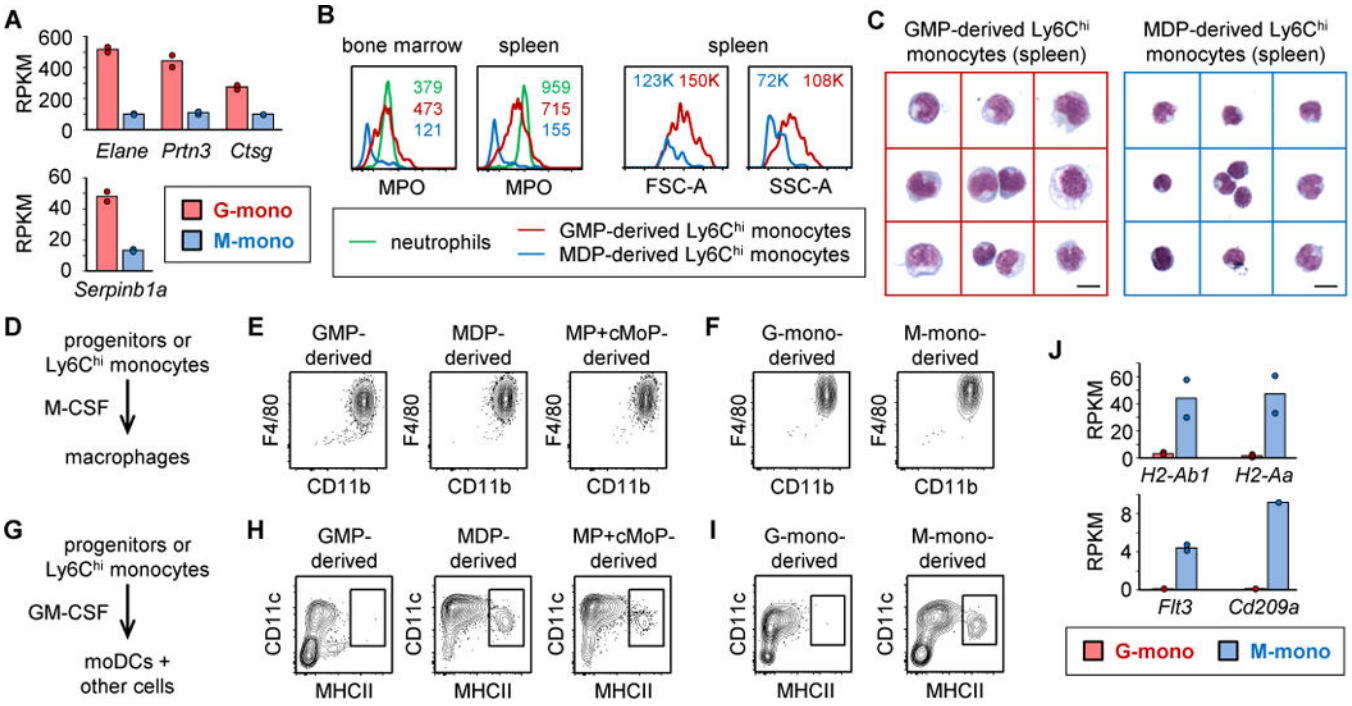

Figure 5. GMPs yield "neutrophil-like" Ly6C^{hi} monocytes, and MDPs give rise to moDC-producing Ly6C^{hi} monocytes

(A) Granule gene expression by GMP- and MDP-derived Ly6C^{hi} monocytes (G-mono and M-mono respectively; data are from the bulk RNA sequencing dataset). (B–C) CFSE-stained GMPs and MDPs were adoptively transferred into recipient mice, and spleens were harvested 3 days later. MPO expression plus forward and side scatter (FSC-A and SSC-A) (B) of donor-derived Ly6C^{hi} monocytes (CFSE^{+} CD11b^{+} Ly6G^{-} CD115^{+} Ly6C^{hi}) were assessed by flow cytometry, and FACS-sorted donor-derived Ly6C^{hi} monocytes were visualized by microscopy with May-Grunwald Giemsa staining to assess morphology (C; scale bar 10 μm). (D–F) Macrophage production in cultures of progenitors or Ly6C^{hi} monocytes with 50 ng/ml M-CSF was assessed by flow cytometry. (E) GMPs, MDPs and the mixed MP+cMoP fraction of bone marrow were cultured with M-CSF for 7 days (E). (F) Ly6C^{hi} monocytes FACS-sorted from 3-day M-CSF cultures of GMPs and MDPs (G-monos and M-monos, respectively) were cultured with M-CSF for a further 4 days. (G–I) moDC (CD11c^{+} MHCII^{hi} cells) production in cultures of progenitors or Ly6C^{hi} monocytes with 20 ng/ml GM-CSF was assessed by flow cytometry. (H) GMPs, MDPs and the mixed MP +cMoP fraction of bone marrow were cultured with GM-CSF for 7 days. (I) Ly6C^{hi} monocytes FACS-sorted from 3-day M-CSF cultures of GMPs and MDPs (G-monos and M-monos, respectively) were cultured for a further 4 days with GM-CSF. Data are representative of at least 3 independent experiments. (J) Expression of MHCII genes (*H2-Ab1* and *H2-Aa*), *Flt3* and *CD209a* by GMP- and MDP-derived Ly6C^{hi} monocytes (G-mono and M-mono, respectively; data are from the bulk RNA sequencing dataset).

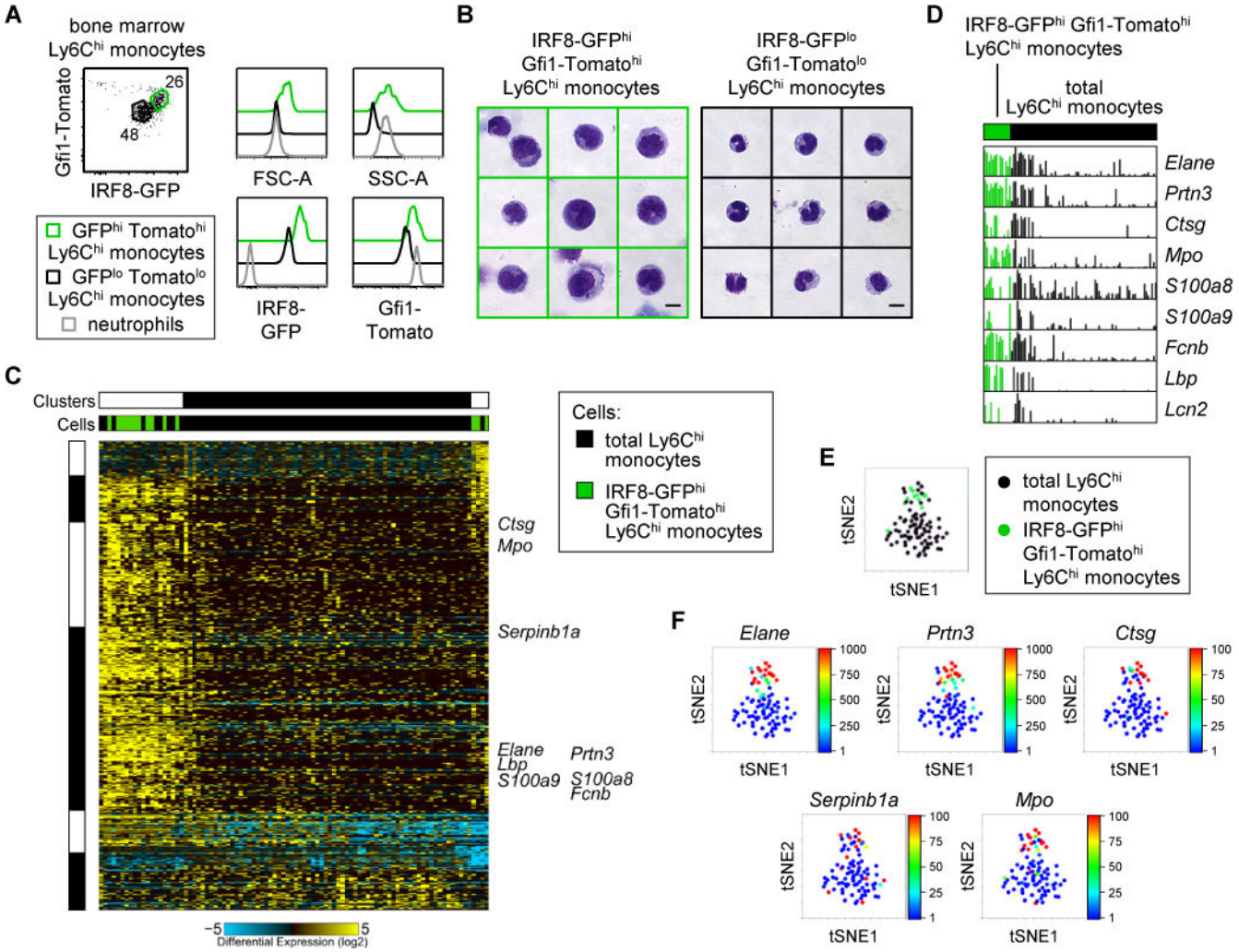

Figure 6. Single-cell RNA sequencing reveals a subset of "neutrophil-like" Ly6C^{hi} monocytes in mouse bone marrow

(A–B) Ly6C^{hi} monocytes were isolated from IRF8-GFP Gfi1-tdTomato reporter mice, profiled by flow cytometry in comparison with neutrophils (A), and visualized by microscopy with May-Grunwald Giemsa staining to assess morphology (B). (C–F) Total Ly6C^{hi} monocytes from wild-type mice (78 monocytes isolated from bone marrow pooled from 5 mice) and GFP^{hi} Tomato^{hi} Ly6C^{hi} monocytes from IRF8-GFP Gfi1-tdTomato reporter mice (14 monocytes isolated from bone marrow pooled from 3 mice) were profiled by single-cell RNA sequencing. (C) AltAnalyze profiling of individual Ly6C^{hi} monocytes using 1309 genes correlated (rho>0.04) to the expression of 123 genes identified as differentially expressed in the bulk RNA sequencing analysis (G-mono^{UP} vs. M-mono^{UP}; only ICGS expressed genes were considered). (D) Comb plots of neutrophil granule gene expression by individual Ly6C^{hi} monocytes. (E–F) The single-cell RNA sequencing data was also analyzed using Cytobank. (E) The monocytes were clustered using 252 genes that were differentially expressed in GMP- and MDP-derived Ly6C^{hi} monocytes (G-mono^{UP} and M-mono^{UP} genes identified by bulk sequencing) and also detected by single-cell RNA

sequencing; tSNE plots are shown. (F) Expression intensities (log10 RPKM) of neutrophil granule genes are shown overlaid on the tSNE plots.

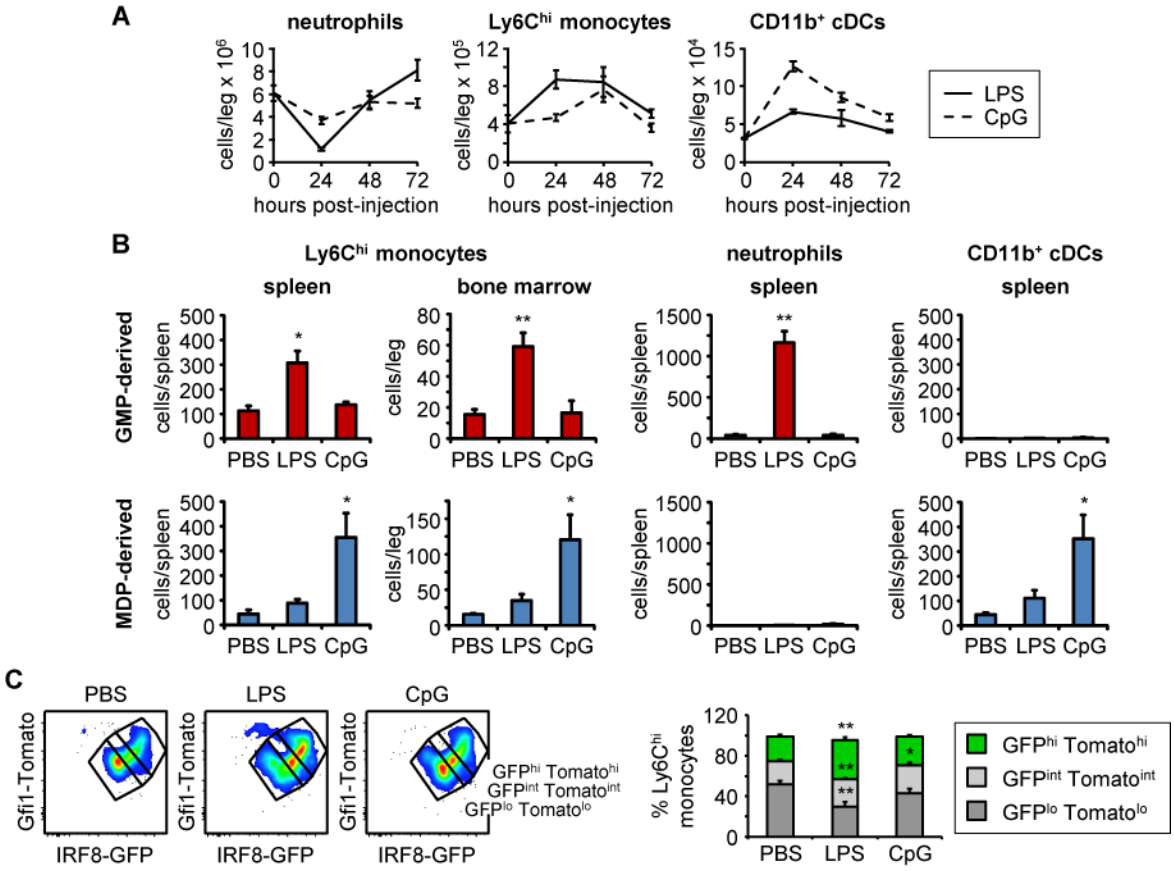

Figure 7. LPS and CpG treatment differentially mobilize GMPs and MDPs *in vivo*

(A) LPS (25 μg/mouse) or CpG (5 μg/mouse) + DOTAP (25 μg/mouse) was injected i.v. into mice, and neutrophils, Ly6C^{hi} monocytes and CD11b^{+} cDCs in the bone marrow were assessed at the indicated timepoints post-injection. Data are presented as means plus standard deviation of 3 mice/group and are representative of at least 2 independent experiments. (B) 25,000 GMPs or MDPs isolated from CD45.2 donor mice were injected i.v. into CD45.1 recipient mice (non-irradiated) on day 0. LPS (25 μg/mouse) or CpG (5 μg/mouse) + DOTAP (25 μg/mouse) was injected i.v. into the mice 2 hours later. Bone marrow and spleens were harvested from recipient mice 3 days after progenitor injection, and splenocytes were enriched for CD45.2^{+} (donor-derived) cells prior to staining for flow cytometry to detect donor cell-derived Ly6C^{hi} monocytes, neutrophils and CD11b^{+} cDCs. Data are presented as mean plus standard error of 3 mice that received progenitors in independent experiments. (C) LPS (25 μg/mouse) or CpG (5 μg/mouse) + DOTAP (25 μg/mouse) was injected i.v. into IRF8-GFP Gfi1-tdTomato reporter mice, and Ly6C^{hi} monocytes in the bone marrow were assessed 48 hours later. Data are presented as means plus standard deviation of 3 mice/group. Statistical significance was assessed by Student's t-test (*p<0.05, **p<0.01).